Noncell-autonomous photoreceptor degeneration in a zebrafish model of choroideremia

Bryan L. Krock*, Joseph Bilotta†‡, and Brian D. Perkins*§

*Department of Biology, Texas A & M University, College Station, TX 77843; and †Department of Psychology and Biotechnology Center, Western Kentucky University, Bowling Green, KY 42101

Edited by John E. Dowling, Harvard University, Cambridge, MA, and approved January 10, 2007 (received for review July 11, 2006)

Choroideremia is an X-linked hereditary retinal degeneration resulting from mutations in the Rab escort protein-1 (*REP1*). The Rep1 protein facilitates posttranslational modification of Rab proteins, which regulate intracellular trafficking in the retinal pigment epithelium (RPE) and photoreceptors and are likely involved in the removal of outer segment disk membranes by the RPE. A critical question for potential treatment of choroideremia is whether photoreceptor degeneration results from autonomous defects in opsin transport within the photoreceptor or as a nonautonomous and secondary consequence of RPE degeneration. To address this question, we have characterized the retinal pathology in zebrafish *rep1* mutants, which carry a recessive nonsense mutation in the *REP1* gene. Zebrafish *rep1* mutants exhibit degeneration of the RPE and photoreceptors and complete loss of visual function as measured by electroretinograms. In the mutant RPE, photoreceptor outer segment material was not effectively eliminated, and large vacuoles were observed. However, opsin trafficking in photoreceptors occurred normally. Mosaic analysis revealed that photoreceptor degeneration was nonautonomous and required contact with the mutant RPE as mutant photoreceptors were rescued in wild-type hosts and wild-type photoreceptors degenerated in mutant hosts. We conclude that mutations in *REP1* disrupt cellular processes in the RPE, which causes photoreceptor death as a secondary consequence. These results suggest that therapies that correct the RPE may successfully rescue photoreceptor loss in choroideremia.

retinal degeneration | retinal pigment epithelium

Choroideremia (CHM) is an X-linked form of retinal degeneration caused by mutations in the gene for Rab escort protein 1 (Rep1) (1, 2), a protein found in all tissues and highly expressed in the outer retina and retinal pigment epithelium (RPE). CHM causes night blindness in children and progresses to complete loss of vision in adults. CHM is one of the few hereditary blindness disorders that can be clinically identified before significant loss of visual function (3), suggesting that diagnosis and intervention during childhood may prevent further loss of vision.

Rep proteins play an essential role in the posttranslational modification of Rab proteins, the small GTP-binding proteins that are essential for many aspects of intracellular transport. Rep proteins bind newly synthesized Rab proteins and facilitate the addition of geranyl-geranyl groups, a modification essential for Rab function in intracellular trafficking (reviewed in ref. 4). In humans, Rep1 and its homolog, Rep2, are ubiquitously expressed and exhibit overlapping substrate specificity (5). Mutations in Rep1 prevent the modification of Rab proteins, thereby disrupting Rab-mediated intracellular trafficking in photoreceptors and the RPE. Because patients with CHM only experience age-related blindness, Rep2 appears to effectively compensate for the loss of Rep1 in all tissues except the eye (6). Interestingly, zebrafish do not contain a Rep2 ortholog, and the loss of Rep1 results in lethality at larval stages (7).

The development and survival of photoreceptors requires effective intracellular trafficking in both photoreceptors and the RPE. In the photoreceptor, proteins destined for the outer segment (e.g., opsin) travel from the Golgi to the connecting cilium via vesicular transport that is regulated by Rab8 and Rab6 (8, 9). In *Xenopus laevis* expressing dominant-negative forms of Rab8, rapid photoreceptor degeneration and defects in outer segment morphogenesis were observed (10). It has been proposed that mutations in Rep1 may lead to defects in opsin trafficking that contribute to photoreceptor degeneration (11). In the RPE, intracellular trafficking controls the phagocytosis and degradation of disk membranes shed from the apical tips of photoreceptor outer segments. Failure of the RPE to clear outer segment debris leads to a toxic environment surrounding the photoreceptors and causes death. It is believed that Rab proteins function during phagocytosis by the RPE, although the mechanism is not clear. It is known that Rab27a is a target of Rep1 and that Rab27a interacts with myosin VIIA in the transport of melanosomes (12, 13). Furthermore, cultured RPE cells that lack myosin VIIA exhibit defects in the phagocytosis of outer segment membranes (14). A tempting hypothesis states that loss of Rep1 disrupts the function of a Rab27a–myosinVIIA complex and causes defects in phagocytosis by the RPE. Because all retinal cells express Rep1, it is unknown whether CHM reflects a cell-autonomous degeneration of photoreceptors, a noncell-autonomous effect caused by RPE dysfunction, or a combination of both. Development of appropriate therapies requires a clear understanding of the tissue-specific contributions to disease.

Here, we report that zebrafish carrying a recessive nonsense mutation in *rep1* (7) exhibit retinal phenotypes consistent with CHM. Using histological, functional, and embryonic manipulations, we found that *rep1* mutants experience photoreceptor degeneration, loss of visual function, and defects in RPE pigmentation and outer segment phagocytosis. By producing genetically mosaic animals, we show that the loss of Rep1 in the RPE is sufficient to induce degeneration of wild-type photoreceptors. These findings provide insight into the pathology of the disease and have implications for the design of future therapies.

Results

The morphological phenotypes of *rep1* mutants have been described (7), but retinal defects have not been studied extensively. Mutants had slightly smaller eyes, and the loss of pigment in the RPE could be observed through the lens as a cloudy coloration in the posterior part of the eye (data not shown). Because patients with CHM lose vision, an animal model of

Author contributions: B.L.K., J.B., and B.D.P. designed research; B.L.K., J.B., and B.D.P. performed research; B.L.K., J.B., and B.D.P. analyzed data; and B.D.P. wrote the paper.

The authors declare no conflict of interest.

This article is a PNAS direct submission.

Freely available online through the PNAS open access option.

Abbreviations: dfp, days postfertilization; RPE, retinal pigment epithelium; CHM, choroideremia; ERG, electroretinogram; Rep1, Rab escort protein 1.

‡Deceased January 2, 2006.

§To whom correspondence should be addressed. E-mail: bperkins@mail.bio.tamu.edu.

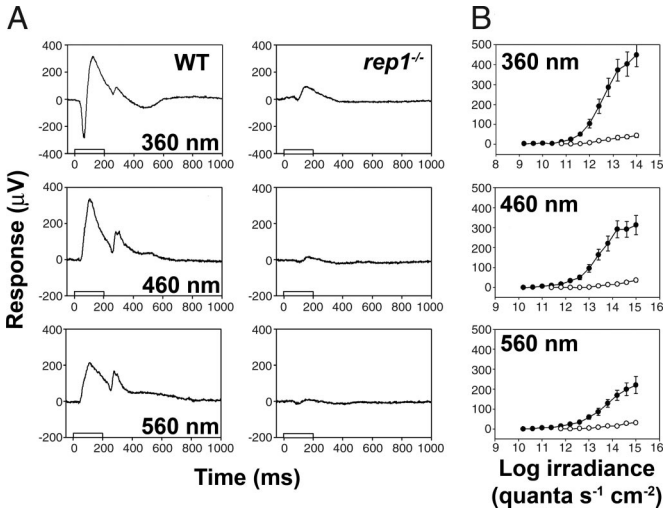

Fig. 1. ERG analysis of *rep1* mutant larvae. (*A*) ERG responses from 5 dpf wild-type (*Left*) and mutant (*Right*) to 200-msec flashes of light at the designated wavelengths. Each waveform was based on the average response from 10 stimulus presentations. Stimulus irradiance (15 log quanta $s^{-1}{\cdot}cm^{-2}$) was the same across all panels. Bars represent the light stimulus. (*B*) Graph of the average irradiance-response functions from wild-type (filled circles; $n = 11$) and mutant (open circles; $n = 14$) subjects based on the b-wave amplitude at three different wavelengths. Error bars represent ±1 SEM. A mixed-design ANOVA found a significant difference ($P \leq 0.05$) between the wild-type and mutant responses at the last five irradiances tested.

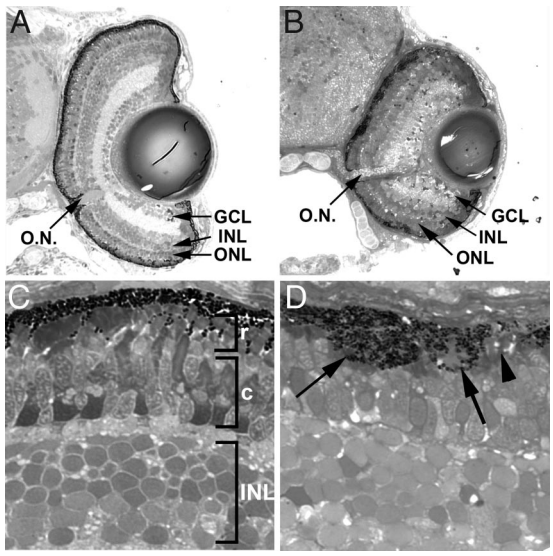

Fig. 2. Histological sections of 4.5 dpf wild-type and *rep1* mutant retinas. (*A*) Wild-type retinas at 4.5 dpf have fully laminated and retinal ganglion cells (GCL), amacrine and bipolar interneurons (INL), and photoreceptors (ONL) differentiated, and the optic nerve (O.N.) is apparent. (*B*) Lamination and cellular differentiation is not affected in *rep1* mutants, but eye size is reduced and the RPE layer appears irregular. (*C*) High magnification of sections from light-adapted wild-type retinas showing the rod (r) outer segments positioned distally from the cone (c) outer segments. (*D*) Sections of *rep1* mutants showing areas of RPE hypertrophy (arrows) into the photoreceptor layer and other regions where the RPE is almost devoid of pigmentation (arrowhead). Rod and cone outer segments are not normally positioned and are shorter than wild-type.

CHM should also exhibit visual defects. We used full-field electroretinogram (ERG) recordings to determine whether the *rep1* mutation also results in loss of visual function. We recorded the ERG at 5 days postfertilization (dpf) using stimuli at three different wavelengths (Fig. 1*A*). When presented with a long-flash (≥200 msec), the vertebrate ERG is characterized by a hyperpolarizing a-wave, a depolarizing b-wave, and a depolarizing d-wave, which reflect photoreceptor cell and on- and off-activity of second-order cells, respectively; >360 nm the amplitude of the b-wave masks the a-wave signal. Compared with wild-type animals, all components of the mutant ERG were significantly reduced at 360, 460, and 560 nm. The minimum light intensity required to produce the smallest detectable ERG response was almost two orders of magnitude higher in the mutants depending on the wavelength tested (Fig. 1*B*). The b-wave amplitude of *rep1* mutants was reduced across a range of stimuli intensities at all three wavelengths. These data indicate that *rep1* mutants exhibit severe loss of outer retina function.

CHM is characterized by degeneration of the choroid, RPE, and photoreceptors, so we investigated the retinal histology of *rep1* mutants. Retinal lamination of *rep1* mutants was not affected, and all major cell types were present (Fig. 2). The RPE maintains a consistent thickness in wild-type animals; however, RPE thickness was highly irregular in the mutants. Hypertrophic areas extended into the photoreceptor layer, and other areas possessed few or no observable melanosomes. The morphology of the mutant photoreceptor layer was disorganized. Mutant photoreceptor outer segments were compressed against hypertrophic regions of RPE. In wild-type retinas, rod and cone photoreceptors are tiered, with UV cones located basally and rods located apically. In *rep1* mutant retinas, no discernable tiering could be observed, perhaps due to hypertrophy of the RPE into the photoreceptor layer.

Ultrastructural analysis of *rep1* mutants by transmission electron microscopy revealed additional defects of the photoreceptors and RPE (Fig. 3). In *rep1* mutants, photoreceptor outer segments were disheveled and degenerating. Melanosomes in the RPE cells were smaller and more immature than those found in wild-type animals. Large vacuoles and undigested outer segment disk membranes were observed within the RPE of the

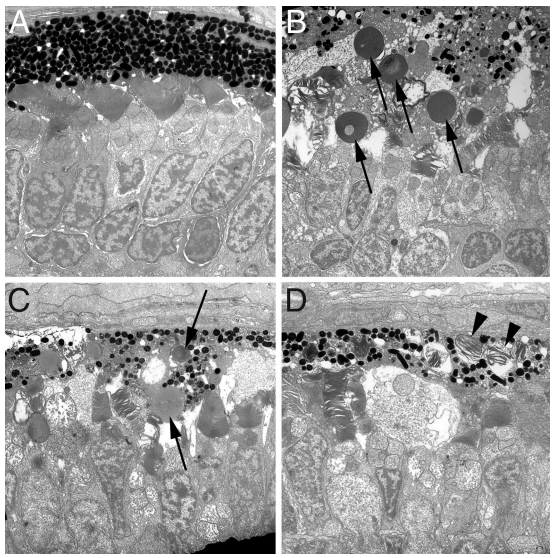

Fig. 3. Transmission electron microscopy of 4.5 dpf wild-type and *rep1* mutant retinas. (*A*) Electron micrographs of wild-type retinas reveal an orderly array of photoreceptor outer segments and the uniform thickness of the RPE. Melanosome maturation within the RPE is normal. (*B–D*) Electron micrographs from multiple *rep1* retinas showing degeneration of the RPE and photoreceptors. Arrows in *B* and *C* indicate large vacuoles observed in the RPE of *rep1* mutants. Arrowheads in *D* indicate outer segment material not digested by the RPE. Melanosome size and maturation vary more dramatically and are less dense than what is seen in wild type.

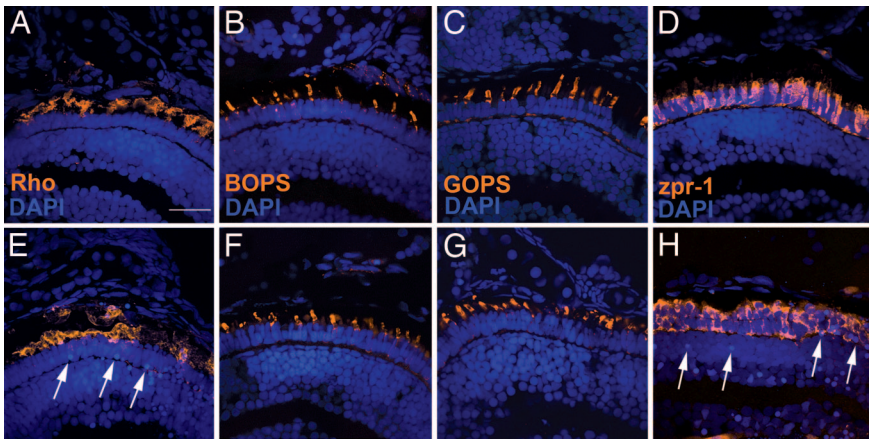

Fig. 4. Opsin trafficking is unaffected in *rep1* mutants. Retinal cryosections were stained with markers for rod and cone photoreceptors in wild type (*A–D*) and *rep1* mutants (*E–H*). The 1D1 marker labels rhodopsin (Rho), whereas antibodies are against blue opsin (BOPS) and green opsin (GOPS) in the photoreceptor outer segments of wild-type and *rep1* mutants. The zpr-1 antibody labels the red/green double cones and reveals the disheveled morphology of the photoreceptors. All sections were counterstained with DAPI to visualize nuclei. Pyknotic nuclei, a hallmark of cell death, are seen in *rep1* mutants and indicated by arrows. (Scale bar, 20 μm.)

mutants. The results from light microscopy and electron microscopy indicate that loss of Rep1 disrupts maturation of melanosomes and the elimination of photoreceptor disk membranes within the RPE and leads to degeneration of the RPE and photoreceptors.

It is well established that defects in opsin trafficking can lead to photoreceptor death. Because Rab proteins function in opsin trafficking (8–10), we tested the hypothesis that loss of Rep1 results in opsin mislocalization and therefore contributes to degeneration in CHM. Retinal sections labeled with an antibody that recognizes rhodopsin (1D1) showed little to no mislocalization in wild-type or mutant rods (Fig. 4 *A* and *E*). During development, small amounts of rhodopsin can be seen around the plasma membrane in wild-type rods (15, 16), and this was occasionally observed in *rep1* mutants, although this was not interpreted as an effect of Rep1 loss. In addition, both blue and green cone opsin proteins localized exclusively to the cone outer segments in wild-type and mutant animals (Fig. 4 *B*, *C*, *F*, and *G*). Taken together, these data indicate that opsin mislocalization is not responsible for photoreceptor degeneration.

Because the larval ERG is cone-dominated, we used additional immunohistochemical markers to specifically investigate cone morphology. In wild-type animals, the red/green double cones are regularly spaced and columnar in appearance (Fig. 4 *D* and *H*). In *rep1* mutants, these cones are irregularly shaped, appear disheveled, and have lost their columnar organization. To determine whether photoreceptor synapses were affected in *rep1* mutants, retinas were stained with antibodies for a glutamate transporter, GLT-1, which stains cone pedicles and bipolar cell terminals in goldfish, and the outer plexiform layer of zebrafish (17, 18). We found that GLT-1 labeling was missing from the outer plexiform layer and strongly reduced in the inner plexiform layer, suggesting that cone degeneration disrupts synapse formation and may have deleterious effects on inner retinal cells such as bipolar cells (Fig. 5). Although correlative, loss of GLT-1 immunoreactivity agrees with the loss of activity by inner retinal cells seen in the ERG of *rep1* mutants.

In *rep1* mutant zebrafish, the degenerating RPE fails to eliminate photoreceptor disk membranes, and yet transport of opsin within the photoreceptors is normal. We therefore addressed the hypothesis that photoreceptor degeneration is non-cell-autonomous and directly caused by the RPE. We produced genetically mosaic eyes in *rep1* and wild-type animals by transplanting cells from blastula stage embryos (19). Cells from donor embryos that had been injected with a lineage tracing dye (rhodamine-dextran) were transplanted into unlabeled hosts. Transplanted cells gave rise to clones of varying size that were assessed for cone morphology and cell death. Wild-type cells transplanted into wild-type hosts produced cones with normal morphology with no evidence of cell death (Fig. 6 *A–D*). When *rep1* mutant cells were transplanted into *rep1* mutant hosts, the photoreceptors produced by the clones lacked the columnar organization and were similar in morphology to cells outside the clone (Fig. 6 *M–P*). In addition, cell death was often observed within and outside the clone as small, round pyknotic nuclei that stained brightly with DAPI. When mutant cells were transplanted into wild-type hosts, the photoreceptor morphology was rescued, and cell death was rarely observed anywhere within the clone (Fig. 6 *E–H*). Conversely, when wild-type cells were transplanted into mutant hosts, cell death was observed within the clone and the morphology of photoreceptors within the wild-type clone resembled that of the surrounding mutant cells (Fig. 6 *I–L*). Quantification of clones exhibiting cell death revealed that almost all clones of mutant photoreceptors (94%) could be rescued when placed opposite wild-type RPE (Table 1). Importantly, most clones of wild-type cells (71%) exhibited some cell death and acquired an abnormal morphology when placed opposite RPE from mutant animals.

To directly test the role of mutant RPE in photoreceptor dysfunction, we transplanted cells from wild-type or *rep1* mutant donors into albino hosts (Fig. 7). Because donor cells were pigmented, the location of RPE clones was easily identified in the albino hosts. Photoreceptor morphology remained unaffected by the presence of wild-type RPE, and no differences could be seen

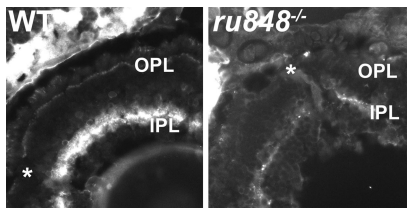

Fig. 5. Loss of *rep1* disrupts photoreceptor termini. Retinal cryosections of wild type (*Left*) and *rep1* mutant (*Right*) retinas were stained with an antibody against the glutamate transporter (GLT-1). Staining in the OPL and IPL is greatly reduced in *rep1* mutants. The asterisks mark the optic nerve.

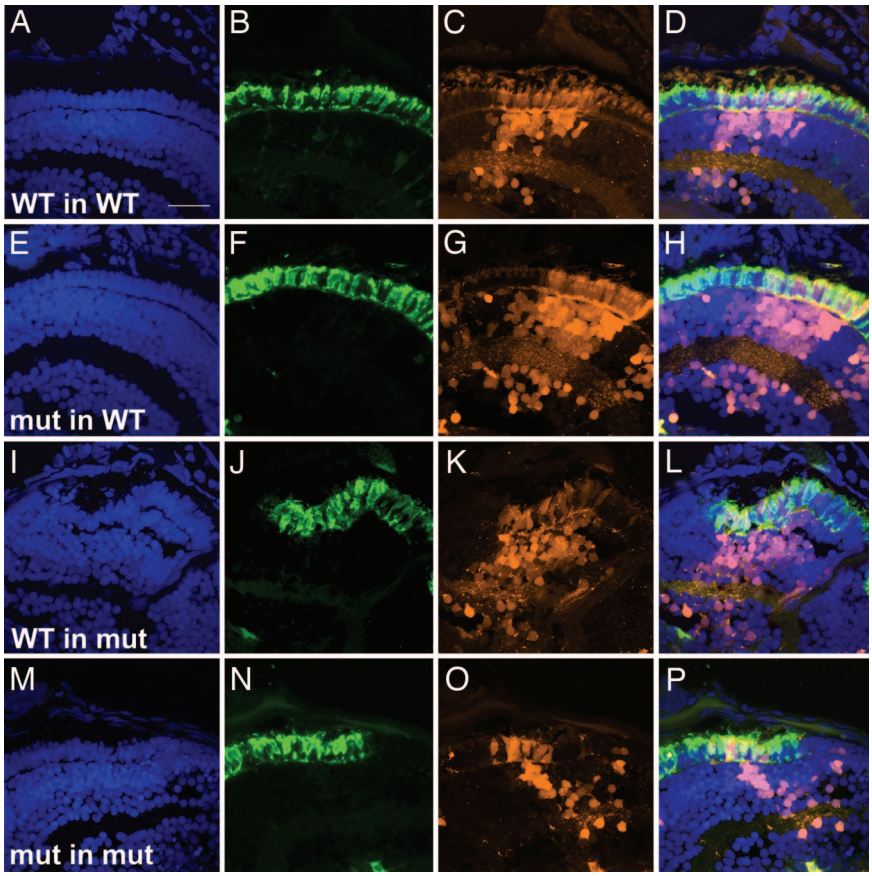

Fig. 6. Analysis of photoreceptor morphology and survival in mosaic animals (see text for details). Genetically mosaic animals were created by blastomere transplantation. Shown are retinal cryosections of 4.5 dpf mosaic animals. Cryosections were stained with DAPI to visualize nuclei (blue; *A*, *E*, *I*, and *M*) and the zpr-1 antibody to label the red-green double cones (green; *B*, *F*, *J*, and *N*). Donor cells were labeled by the lineage-tracer rhodamine-dextran (red cells; *C*, *G*, *K*, and *O*). Composite images (*D*, *H*, *L*, and *P*) show all markers and labels. (Scale bar, 20 μm.)

in photoreceptors in contact with the RPE clone and those outside the clone (Fig. 7 *A–E*). In contrast, RPE cells from *rep1* mutant donors disrupted the morphology of the host photoreceptors. The host photoreceptors were shorter, disheveled, and more disorganized than those photoreceptors not in contact with the mutant RPE clone (Fig. 7 *F–J*). Taken together, the mosaic experiments show that photoreceptor degeneration in CHM is noncell-autonomous and RPE cells lacking Rep1 are both necessary and sufficient for photoreceptor cell death.

Discussion

The purpose of this study was to investigate the retinal pathology of a zebrafish model of CHM and to test various hypotheses regarding the mechanism of photoreceptor degeneration. The results point to four significant findings. First, mutation of the zebrafish *rep1* gene caused degeneration of the RPE and photoreceptors in a manner that closely resembled the degeneration seen in human cases of CHM (20). Similar to what is observed in human cases of CHM (21, 22), zebrafish *rep1* mutants exhibit variable thickness of the RPE, with areas of depigmentation and accumulation of outer segment material in the RPE. Mutant photoreceptors became much shorter, and visual function was highly reduced or absent. Thus, the zebrafish represents a suitable animal model for this disease. Second, the RPE of *rep1* mutant zebrafish failed to properly eliminate photoreceptor disk membranes, which can be a cause of nonautonomous photoreceptor death (23). The failure to effectively digest phagosomes carrying disk membranes is hypothesized to cause the accumulation of lipofuscin within the RPE, which is a clinical feature of CHM, and other forms of retinal degeneration (20, 24, 25). Third, opsin mislocalization was not observed in intact rod or cone photoreceptors. Mislocalization of opsin was observed in a single case study of a female carrier of CHM in which photoreceptor degeneration was variable (20). Although mutations that affect rhodopsin folding and trafficking can cause autonomous photoreceptor cell death (10, 26–28), opsin mislocalization can also occur when the RPE fails to phagocytize shed disk membranes, as in the RCS rat (29, 30) and possibly in the Myo7a mouse (14). Finally, genetic mosaic analysis indicated that the RPE of *rep1* zebrafish was both necessary and sufficient to cause photoreceptor degeneration (Figs. 6 and 7).

Perhaps the most debated question regarding the pathology of CHM is the primary site of the disease. Our results strongly suggest that photoreceptor death in CHM is secondary to defects in the RPE, which differs from previous studies. In reports of a human female carrier of CHM (20) and CHM mouse models (31), the authors argue that the severity of degeneration of photoreceptors and RPE does not always correlate, suggesting

Table 1. Cell death within mosaic clones

	Clones analyzed	Clones with pyknotic nuclei
WT→WT	12	0 (0%)
mut→WT	16	1 (6%)
WT→mut	17	12 (71%)
mut→mut	6	5 (83%)

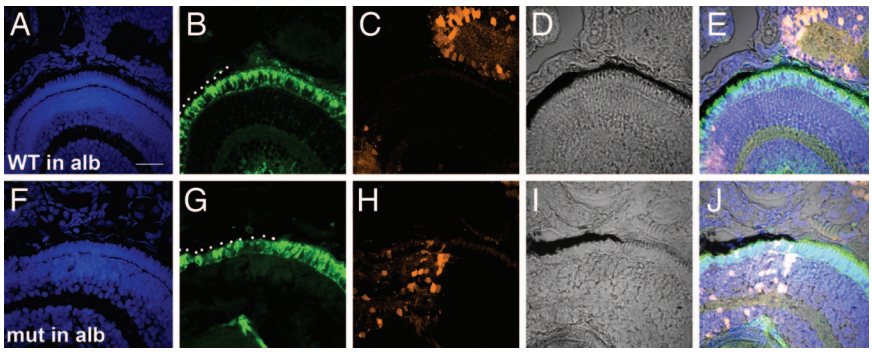

Fig. 7. Effects of RPE clones on wild-type photoreceptor morphology. Donor cells from wild-type or *rep1* mutant embryos were transplanted into albino hosts to visualize transplanted RPE clones. Retinal cryosections of 4.5 dpf mosaic animals were stained with DAPI to visualize nuclei (blue; *A* and *F*) and the zpr-1 antibody to label the red-green double cones (green; *B* and *G*). Donor cells were labeled by the lineage-tracer rhodamine-dextran (red cells; *C* and *H*). Bright-field images using Nomarski optics (*D* and *I*) were used to visualize and distinguish pigmented RPE (donor) from albino RPE (host). Composite images (*E* and *J*) show all markers and labels. The dotted line (*B* and *G*) denotes the location of donor RPE. (Scale bar, 20 μm.)

that the tissues degenerate independently. To address the autonomy of the disease, Tolmachova *et al.* (31) bred mice carrying a Chm^{flox} gene with mice carrying a *six3-Cre* transgene to generate a tissue-specific knockout of the mouse *CHM* gene. During development, however, both *six3* and *six3-Cre* transgenes are expressed in the anterior neural plate and the optic vesicle, which are tissues that give rise to both neural retina and RPE (32, 33). Thus, autonomy could not be directly tested in these experiments because the *CHM* gene was likely missing from both photoreceptors and RPE. Our results and methodology are similar to those of Mullen and LaVail (34), who used chimeric animals to identify the RPE as the primary site of disease in RCS rats. It should be noted that the long-term fate of mutant photoreceptors in our mosaic animals is not known, and we cannot rule out the possibility that a slow, progressive degeneration may occur. Furthermore, because zebrafish lack an ortholog to the human Rep2 protein, the effects observed in this study may be more severe than what occurs in human CHM patients. Nevertheless, our results show that loss of Rep1 from the RPE is sufficient for early photoreceptor degeneration in zebrafish. These results have significant implications on the development of appropriate RPE-specific therapies to treat and correct CHM. Because this disease can be diagnosed during childhood while symptoms are mild (3), effective intervention of the RPE at early ages may prevent loss of vision later in life.

Materials and Methods

Zebrafish Care and Maintenance. The $rep1^{ru848}$ allele, which contains a nonsense mutation (Q32X) in the second exon, was obtained from James Hudspeth, The Rockefeller University, New York (7). Albino animals were obtained from the Zebrafish International Resource Center. All fish were maintained according to standard methods (35).

Histology: Light Microscopy and Transmission Electron Microscopy. Embryos were processed for histology as described (36). For transmission electron microscopy, transverse sections (60–80 nm) of the central retina were stained with lead citrate and uranyl acetate. Photographs were obtained with a transmission electron microscope (JEOL, Tokyo, Japan), and image processing was performed by using Photoshop (Adobe Systems, Mountain View, CA).

Immunohistochemistry. Immunohistochemistry was performed as described (15). Images were obtained with an FV1000 confocal microscope (Olympus, Tokyo, Japan). The following is a list of primary antibodies used, dilution, and cell types that possess the antigens: 1D1 (1:500) rods (37), Zpr1 (1:100) red-green double cones (38), cone opsin antibodies (1:200) (39), and glutamate transporter (1:100; AB1783, Chemicon, Temucula, CA) (17). The appropriate fluorescently conjugated antibodies (Jackson ImmunoResearch Laboratories, West Grove, PA) were used at 1:500 dilutions. Slides were counterstained with DAPI (Molecular Probes, Eugene, OR) to label DNA.

Electroretinographic Recording. Details of the optical system and embryo preparation can be found in refs. 40–42. All experiments were performed on light-adapted animals at 5 dpf. Animals were given a 200-ms stimulus at a range of irradiances (10–15 log quanta $s^{-1}{\cdot}cm^{-2}$) at 360-, 460-, and 560-nm wavelengths.

Mosaic Analysis. Mosaic retinas were produced by blastomere transplantation (19). Clutches of embryos from *rep1* heterozygous matings were dechorionated and injected at the one- to four-cell stage with a lineage-tracing label [1:9 mix of lysine fixable rhodamine-dextran (Molecular Probes) at a total concentration of 5% (wt/vol)]. At the 1,000-cell stage, 10–40 donor cells were transplanted to the animal pole of the dechorionated wild-type hosts, and the region was fated for eye and forebrain (43). Donor embryos were phenotyped at 4 dpf, and host embryos were fixed in 4% paraformaldehyde at 4.5 dpf. Donor cells in host embryos were assessed by immunohistochemistry and confocal microscopy as described above.

We thank Jim Hudspeth for providing the $rep1^{ru848}$ mutant line, Tom Vihtelic (University of Notre Dame, Notre Dame, IN) for providing the cone opsin antibodies, Zebrafish International Resource Center for antibodies and animals, and Jeff Gross, Michael Manson, Bruce Riley, and two anonymous reviewers for comments on the manuscript. This work was supported by a Fight For Sight grant (to B.D.P.) and National Institutes of Health Grant P20 RR-16481 (to J.B.).

1. Cremers FP, Sankila EM, Brunsmann F, Jay M, Jay B, Wright A, Pinckers AJ, Schwartz M, van de Pol DJ, Wieringa B, *et al.* (1990) *Am J Hum Genet* 47:622–628.
2. Seabra MC, Brown MS, Slaughter CA, Sudhof TC, Goldstein JL (1992) *Cell* 70:1049–1057.
3. Sorsby A, Franceschetti A, Joseph R, Davey JB (1952) *Br J Ophthalmol* 36:547–581.
4. Preising M, Ayuso C (2004) *Ophthalmic Genet* 25:101–110.
5. Cremers FP, Armstrong SA, Seabra MC, Brown MS, Goldstein JL (1994) *J Biol Chem* 269:2111–2117.
6. Seabra MC (1996) *Ophthalmic Genet* 17:43–46.
7. Starr CJ, Kappler JA, Chan DK, Kollmar R, Hudspeth AJ (2004) *Proc Natl Acad Sci USA* 101:2572–2577.
8. Deretic D, Huber LA, Ransom N, Mancini M, Simons K, Papermaster DS (1995) *J Cell Sci* 108:215–224.

9. Deretic D, Papermaster DS (1993) *J Cell Sci* 106:803–813.
10. Moritz OL, Tam BM, Hurd LL, Peranen J, Deretic D, Papermaster DS (2001) *Mol Biol Cell* 12:2341–2351.
11. Alory C, Balch WE (2001) *Traffic* 2:532–543.
12. Gibbs D, Azarian SM, Lillo C, Kitamoto J, Klomp AE, Steel KP, Libby RT, Williams DS (2004) *J Cell Sci* 117:6473–6483.
13. Seabra MC, Ho YK, Anant JS (1995) *J Biol Chem* 270:24420–24427.
14. Gibbs D, Kitamoto J, Williams DS (2003) *Proc Natl Acad Sci USA* 100:6481–6486.
15. Perkins BD, Nicholas CS, Baye LM, Link BA, Dowling JE (2005) *Dev Dyn* 233:680–694.
16. Morris AC, Fadool JM (2005) *Physiol Behav* 86:306–313.
17. Yazulla S, Studholme KM (2001) *J Neurocytol* 30:551–592.
18. Vandenbranden CA, Yazulla S, Studholme KM, Kamphuis W, Kamermans M (2000) *J Comp Neurol* 423:440–451.
19. Ho RK, Kane DA (1990) *Nature* 348:728–730.
20. Syed N, Smith JE, John SK, Seabra MC, Aguirre GD, Milam AH (2001) *Ophthalmology* 108:711–720.
21. Flannery JG, Bird AC, Farber DB, Weleber RG, Bok D (1990) *Invest Ophthalmol Visual Sci* 31:229–236.
22. Jacobson SG, Cideciyan AV, Sumaroka A, Aleman TS, Schwartz SB, Windsor EA, Roman AJ, Stone EM, MacDonald IM (2006) *Invest Ophthalmol Visual Sci* 47:4113–4120.
23. Vollrath D, Feng W, Duncan JL, Yasumura D, D'Cruz PM, Chappelow A, Matthes MT, Kay MA, LaVail MM (2001) *Proc Natl Acad Sci USA* 98:12584–12589.
24. Weng J, Mata NL, Azarian SM, Tzekov RT, Birch DG, Travis GH (1999) *Cell* 98:13–23.
25. Kolb H, Gouras P (1974) *Invest Ophthalmol* 13:487–498.
26. Li T, Snyder WK, Olsson JE, Dryja TP (1996) *Proc Natl Acad Sci USA* 93:14176–14181.
27. Pazour GJ, Baker SA, Deane JA, Cole DG, Dickert BL, Rosenbaum JL, Witman GB, Besharse JC (2002) *J Cell Biol* 157:103–113.
28. Sung CH, Davenport CM, Nathans J (1993) *J Biol Chem* 268:26645–26649.
29. Nir I, Papermaster DS (1989) *Prog Clin Biol Res* 314:251–264.
30. Dowling JE, Sidman RL (1962) *J Cell Biol* 14:73–109.
31. Tolmachova T, Anders R, Abrink M, Bugeon L, Dallman MJ, Futter CE, Ramalho JS, Tonagel F, Tanimoto N, Seeliger MW, *et al.* (2006) *J Clin Invest* 116:386–394.
32. Oliver G, Mailhos A, Wehr R, Copeland NG, Jenkins NA, Gruss P (1995) *Development (Cambridge, UK)* 121:4045–4055.
33. Furuta Y, Lagutin O, Hogan BL, Oliver GC (2000) *Genesis* 26:130–132.
34. Mullen RJ, LaVail MM (1976) *Science* 192:799–801.
35. Westerfield M (1995) *The Zebrafish Book* (Univ of Oregon Press, Eugene, OR).
36. Schmitt EA, Dowling JE (1999) *J Comp Neurol* 404:515–536.
37. Fadool JM, Fadool DA, Moore JC, Linser PJ (1999) *Invest Ophthalmol Visual Sci* 40(*Suppl*):1251.
38. Larison KD, Bremiller R (1990) *Development (Cambridge, UK)* 109:567–576.
39. Vihtelic TS, Doro CJ, Hyde DR (1999) *Visual Neurosci* 16:571–585.
40. Saszik S, Bilotta J (1999) *Vision Res* 39:1051–1058.
41. Hughes A, Saszik S, Bilotta J, Demarco PJ, Jr, Patterson WF II (1998) *Visual Neurosci* 15:1029–1037.
42. Bilotta J, Saszik S, Sutherland SE (2001) *Dev Dyn* 222:564–570.
43. Kimmel CB, Ballard WW, Kimmel SR, Ullmann B, Schilling TF (1995) *Dev Dyn* 203:253–310.